Probing nonlocal tracer dispersion in flows through random porous media

A. Ding and D. Candela
Physics and Astronomy Department, University of Massachusetts, Amherst, Massachusetts 01003
(Received 26 January 1996)

Pulsed-field-gradient NMR is used to measure tracer dispersion in flow through a porous medium. Data are presented for water flowing through packs of plastic beads at Péclet numbers $0 \leqslant \mathrm{Pe} \leqslant 150$, using strong, fast gradient pulses to measure pore-scale molecular displacements. The transition at $\mathrm{Pe} \sim 1$ from tortuosity-reduced diffusion to dispersion is observed. The data are Fourier transformed to provide a measurement of the wave-number- and frequency-dependent nonlocal dispersion coefficient. The experimental results compare favorably with an approximate calculation of Koch and Brady [J. Fluid Mech. **180**, 387 (1987); Chem. Eng. Sci. **42**, 1377 (1987)]. [S1063-651X(96)08107-X]

PACS number(s): 47.55.Mh, 76.60.−k, 81.05.Rm, 92.60.Ek

I. INTRODUCTION

The dispersion, or spreading out, of tracers carried by fluid flow through a random porous medium is a process of fundamental importance to such fields as chemical engineering, chromatography, hydrology, and environmental science [1]. In the simplest case, dispersion is modeled by effective diffusion coefficients $D_{\parallel}, D_{\perp}$ for tracer motion perpendicular and parallel to the average flow and an initially localized tracer distribution is Gaussian at all later times.

In many important applications, the overall time and distance scales of the flow are far too small for a Gaussian tracer distribution to develop. For example, the residence time distribution for flow through a porous bed typically has a long-time tail which is poorly modeled by a Gaussian [1]. It remains desirable to find statistical measures of the random flow, such as the dispersion coefficients $D_{\parallel,\perp}$, that can be used to predict the (average) time and space evolution of the tracer distribution. One approach to this complex problem is the nonlocal dispersion formalism of Koch and Brady [2]. In this formalism, the configuration-averaged current $\langle \mathbf{J} \rangle$ of tracer at location and time $\mathbf{r}, t$ is related to concentration gradients $\langle \nabla c \rangle$ at other locations and earlier times by a nonlocal generalization of the dispersion coefficient that depends on space and time differences:

$$\langle \mathbf{J}_{\perp}(\mathbf{r},t) \rangle = -\int d\mathbf{r}' dt' D_{\perp}(\mathbf{r}-\mathbf{r}', t-t') \langle \nabla_{\perp} c(\mathbf{r}', t') \rangle, \quad (1)$$

with a similar expression for the parallel current $\langle \mathbf{J}_{\parallel} \rangle$. The typical extent of the nonlocal dispersion coefficients in space and time are the correlation distance and time of the fluid flow through the random medium. These are roughly the pore size and time for fluid to transit a pore for a statistically uniform medium, but much greater for the nonuniform media encountered in many natural situations.

Knowledge of $D_{\parallel,\perp}(\Delta \mathbf{r}, \Delta t)$ permits prediction of the tracer distribution at arbitrary times, for arbitrary initial conditions. In practice, this formalism has seen little application to experiment because the nonlocal dispersion coefficients are difficult to measure using conventional methods, which typically consist of injecting a tracer pulse into one face of a porous sample and observing the time dependence of the concentration in the flow emerging from the opposite face [1]. The development by Hulin and Salin [3] of electrochemical means of generating and detecting tracers has permitted some exploration of the wave-number dependence of the dispersion coefficient.

In this paper, we demonstrate that pulsed-field-gradient NMR can be an effective tool to measure both conventional and nonlocal dispersion coefficients. Rather than use chemical tracers, fluid molecules are ''tagged'' by the transverse components of their nuclear spins. Using NMR methods that have been well developed for other applications, the displacements of molecules both parallel and perpendicular to the average flow are readily measured over wide ranges of time and distance, limited mainly by the relaxation time T_1.

II. EXPERIMENTAL SETUP AND DATA

This work was initially motivated by recent advances in the application of NMR to porous media [4–6]. These methods use diffusive motion of spins to sample the random pore space, providing statistical measures of the geometry such as the static structure factor $S(q)$ with greater spatial resolution than is possible in direct imaging [4]. Diffusive motion can only be probed by NMR over length scales of order $(D_m T_1)^{1/2}$, where D_m is the molecular diffusion coefficient ($\approx 2.3 \times 10^{-5}$ cm^2/s for water). This length scale is never greater than 100 μm and typically less due to the enhanced relaxation rate T_1^{-1} at surfaces. Thus a recent NMR study of porous rocks [6] successfully measured local features (surface area, pore shape) but did not extend to sufficiently long distances to recover the macroscopic tortuosity.

To circumvent the short diffusive length scale, we have applied a forced convection to the fluid. Figure 1 shows some of our NMR data on water filling the pores of a pack of 15-μm-diam plastic beads, both with and without flow. A computer-controlled pump was used to establish a steady flow of water through the bead pack and the standard NMR techniques of signal averaging and phase cycling were used to acquire echo-height data over a wide dynamic range. The data were taken in a 1-T static field, using the pulsed-field-gradient technique with relatively strong, fast gradient pulses (up to 6 T/m, 400-μs duration), as might be used for NMR

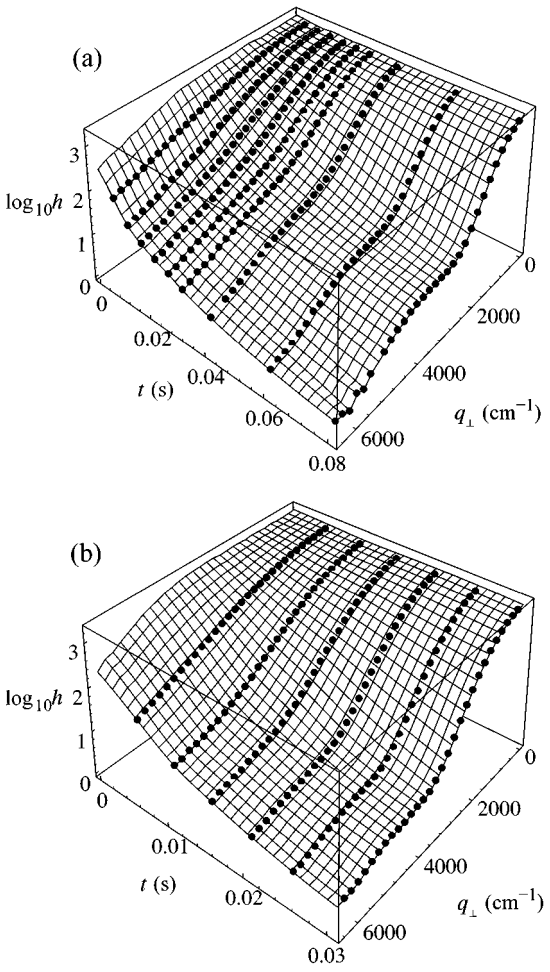

FIG. 1. Experimental NMR echo heights as a function of time and transverse wave number for water filling a pack of 15-μm-diameter plastic beads. In (a) there is no flow. In (b) there is an average flow velocity of 0.088 cm/s corresponding to Péclet number Pe=6. Note the different time scales in the two plots. The solid circles show data points and the surface shows an interpolating function. Wave numbers $q_\perp$ here and in the other figures are in angular units (rad/cm).

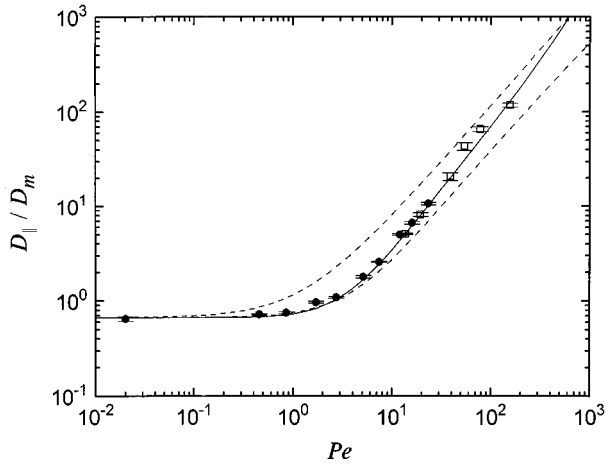

FIG. 2. Longitudinal dispersion coefficient as a function of Péclet number, measured for water flowing through packs of plastic beads of mean diameter 15 μm (filled circles) and 52 μm (open squares). The dispersion coefficient is normalized to the molecular diffusion coefficient D_m, measured on a sample of bulk water in the same apparatus. The data point plotted at Pe=0.02 was actually measured with no flow (Pe=0). The lower dashed curve is a phenomenological fit of Hiby [10] to previous experimental data and the upper dashed curve is our fit to experimental data shown in Fig. 6.16 of Ref. [1]. The solid curve is the theoretical result of Saffman [11] based on a random capillary-network model.

microscopy [7]. A stimulated-echo pulse sequence was used: $\pi/2$-G-$\pi/2$-τ-$\pi/2$-G, where G indicates the gradient pulses and the waiting time τ was varied. The time between the first two $\pi/2$ pulses was kept fixed at a short value, 700 μs. More complex sequences have been developed to reduce the effects of internal gradients in a porous sample [6,8]. In our experiments, the combination of low static field, short transverse evolution periods, and strong gradient pulses effectively reduced the influence of internal gradients without the use of these more complex sequences. This was verified by comparing our lowest-gradient data for diffusion in the bead pack, with data taken on bulk water samples in the same apparatus.

Molecular displacements may be measured parallel or perpendicular to the flow direction, by varying the direction of the gradient pulses; the data we show in Figs. 1 and 2 are for perpendicular and parallel displacements, respectively. In the parallel case, the flow causes a phase shift proportional to time, which can serve as an accurate measure of the average velocity. This phase shift does not interfere with the measurements of dispersion discussed here. While there has been much work on measuring and imaging flow by NMR [9], especially for biological systems, our focus is on the pore-scale physics rather than the macroscopic transport that has typically been of interest. The data with no flow [Fig. 1(a)] resemble the earlier work [4]: at the longest times a plateau develops at wave number $q/2\pi \approx 560$ cm^{-1} or roughly the inverse bead size. Theoretically, the data should evolve as $t \to \infty$ to the structure factor $S(q)$ for a random pack of spheres [4].

When flow is applied [Fig. 1(b)] a similar plateau appears, but at shorter times. This affirms the possibility of obtaining geometric information similar to $S(q)$ in systems where the T_1 limit makes the purely diffusive measurement impossible. It will be noticed from Fig. 1 that the plateau occurs at a slightly higher wave number when flow is applied. This reflects differences in the ''geometry'' of the flow field relative to the geometry of the static pore space, as molecular displacements will be smaller, for example, in stagnant regions. It is not clear why this should move the peak to higher q. For data without flow, $2\pi/q$ at the peak has been interpreted as a particularly likely displacement value for the displacement at long times, and it agrees closely with the typical interpore distance [4]. Within this interpretation our data suggest that the most probable molecular displacement is shortened by flow and we speculate that this reflects the concentration of streamlines toward the centers of pores. The *average* displacement at fixed time is, of course, increased by flow. Below we develop a different way of displaying this long-time,

high-wave-number data, using the ideas of nonlocal dispersion theory.

III. ORDINARY (LOCAL) DISPERSION COEFFICIENTS

Before applying the nonlocal theory, we show that this type of NMR data may be used to extract the ordinary (local) dispersion coefficients $D_{\parallel,\perp}$. These correspond to the large distance, long-time limit and are obtained by fitting the low-q data to $h(q_{\parallel,\perp},t)\approx h(0,0)\exp(-D_{\parallel,\perp}q_{\parallel,\perp}^2 t)$. Figure 2 shows some data for $D_\parallel$ that we have obtained by fitting the data as a function of q at fixed, large t. A discussion of the t dependence is beyond the scope of the present paper; we note only that in the presence of flow the dispersion coefficient *increases* with time to its limiting value, unlike the no-flow diffusion coefficient which *decreases* with time [5].

A dimensionless measure of the importance of flow relative to diffusion is the Péclet number $\mathrm{Pe}=vl/D_m$, where v is the average flow velocity and l is a characteristic length, which we take as the bead diameter. The data shown in Figs. 1 and 2 were taken at relatively low Péclet numbers to show the crossover from pure diffusion, but in principle the present method can be extended to higher Péclet numbers to explore to the complete velocity dependence of holdup, boundary-layer, and mechanical contributions to dispersion [1–3]. The ratio of Péclet to Reynolds numbers is Pe/Re ≈ 400 for water, so all of the data presented here are in the viscous-flow regime $\mathrm{Re}<1$. As shown in Fig. 2, the values of $D_\parallel$ obtained here are consistent with those measured using more conventional means [1,10]. The data for $\mathrm{Pe}\ll 1$ asymptotically approach to a value approximately 30% less than D_m, due to the tortuosity of the pore space.

IV. MEASURING NONLOCAL DISPERSION

We next describe how the nonlocal dispersion coefficient may be obtained from NMR data. The convolution integral of Eq. (1) becomes a simple multiplication under space-time Fourier transformation [2], so the quantity of interest is the Fourier transform of $D_{\parallel,\perp}(\Delta\mathbf{r},\Delta t)$, which we denote by $\widetilde{D}_{\parallel,\perp}(\mathbf{q},\omega)$. A pulsed-field-gradient NMR experiment effectively probes the time evolution of a concentration field with a well-defined wave vector. In principle the entire nonlocal dispersion function may be obtained by a series of NMR experiments varying the time and gradient pulse strength and direction. For example, the transverse dispersion coefficient for wave vectors perpendicular to the flow direction is computed as

$$\widetilde{D}_\perp(q_\perp,\omega)=[k^2\widetilde{h}(q_\perp,\omega)]^{-1}+i\omega/q_\perp^2, \tag{2}$$

where

$$\widetilde{h}(q_\perp,\omega)=\int_0^\infty [h(q_\perp,t)/h(0,0)]e^{i\omega t}dt \tag{3}$$

is the time Fourier transform of the echo height $h(q_\perp,t)$ normalized to its $(q_\perp,t)=(0,0)$ limit. Equation (2) is easily derived from the definition of the nonlocal dispersion coefficient, Eq. (1), by considering the initial gradient pulse to create a tracer distribution that is a δ function of time multiplied by an oscillatory function of position. The configuration average of Eq. (1) is effectively realized in a NMR experiment as the spatial average over a macroscopic sample. It is equally possible to extract the longitudinal nonlocal dispersion coefficient and to measure delocalization of both dispersion coefficients perpendicular to the displacement direction [e.g., $D_\perp(q_\parallel)$]. The experimental protocol and data analysis required are more complicated in these cases and will be discussed elsewhere [12].

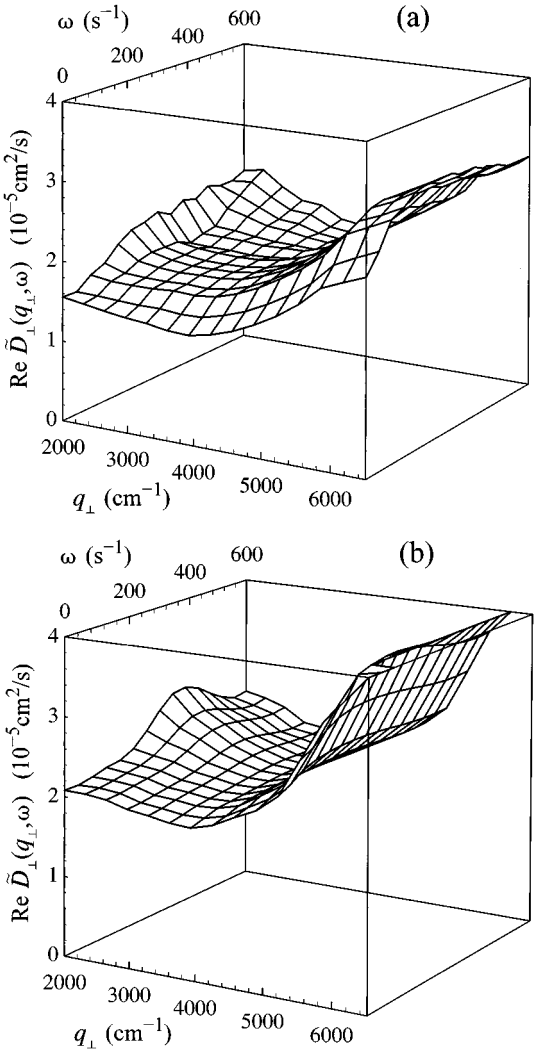

FIG. 3. Nonlocal transverse dispersion coefficient computed from the NMR data shown in Fig. 1 for (a) no flow and (b) average velocity 0.088 cm/s. The real part of $\widetilde{D}_\perp$ is plotted here and in Fig. 4; the imaginary part, which gives rise to a reactive current, is typically smaller than the real part and is not plotted.

In Fig. 3 we show the nonlocal dispersion coefficient computed in this way from the NMR data of Fig. 1. As $\mathrm{Pe}\leqslant 6$ here, $\widetilde{D}_\perp$ is dominated by diffusion in the random pore space, which is itself a complex process. Callaghan *et al.* [4] introduced a ''pore-hopping'' model for the NMR response under purely diffusive (no-flow) conditions, which fit their experimental data on random bead packs. Figure 4(a) shows $\widetilde{D}_\perp(q_\perp,\omega)$ computed from the pore-hopping model, with parameters similar to those of Ref. [4] but scaled to our slightly different bead size. The data [Fig. 3(a)] and the model [Fig.

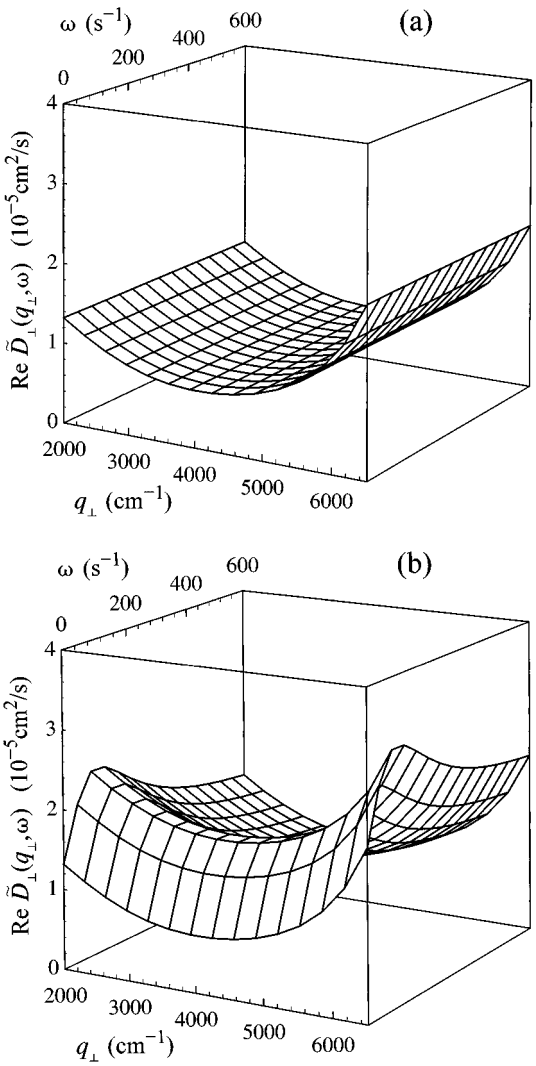

FIG. 4. Model nonlocal transverse dispersion coefficient for (a) no flow and (b) average velocity 0.088 cm/s. For (a), $\widetilde{D}_\perp$ was computed from the ''pore-hopping'' model of Ref. [4]. In (b), the theoretical result of Ref. [2] for mechanical contributions to $\widetilde{D}_\perp(q_\perp,\omega)$ has been added.

4(a)] share some features that may be understood from simple physical arguments: (i) a low-q region where $\mathrm{Re}\widetilde{D}_\perp < D_m$ (tortuosity-reduced diffusion at long distances) and (ii) a high-q region where $\mathrm{Re}\widetilde{D}_\perp \approx D_m$ (free diffusion at short distances). Conversely, $\mathrm{Re}\widetilde{D}_\perp$ is independent of ω in the pore-hopping model, reflecting a simple exponential time dependence of the echo height. This is not true of the data [Figs. 1(a) and 3(a)] and is not predicted by theoretical treatments that take into account restricted diffusion near surfaces [5].

For present purposes, we are more concerned with the *changes* that occur in $\widetilde{D}_\perp$ when flow is applied. The available theoretical calculation of flow contributions to $\widetilde{D}_\perp(\boldsymbol{q},\omega)$ uses the rather severe approximation of the porous medium as a dilute set of noninteracting spheres [2]. In Fig. 4(b) we have added $\widetilde{D}_\perp$ from this calculation to the diffusive $\widetilde{D}_\perp$ of the pore-hopping model, for comparison with the experimental results with flow [Fig. 3(b)]. The calculation gives $\widetilde{D}_\perp \to 0$ as $\omega \to 0$ and consequently a peak at finite ω. These are consequences of the fore-aft symmetry of streamlines about an isolated sphere [2] and thus are neither expected nor seen in experiments on dense bead packs. At low $q_\perp$, the theory is otherwise reasonably close to the experimental results, correctly predicting the approximate magnitude of $\widetilde{D}_\perp$ and its falloff at the largest frequencies probed. At higher $q_\perp$, the experiment shows a strong enhancement with the flow of $\widetilde{D}_\perp$, which is not predicted by the calculation. We believe that this is also a consequence of the approximations made in the calculation, which in fact predicts *no* $q_\perp$ dependence for the mechanical contribution to $\widetilde{D}_\perp$. In the dilute-sphere approximation $\widetilde{D}_\perp$ depends only upon the combination $\omega/v + q_\parallel$ and thus is spatially localized in directions transverse to the average flow [2]. When interactions between the flow fields of adjacent beads are important, as is certainly the case in a dense bead pack, the transverse delocalization of $\widetilde{D}_\perp$ that we observe must be expected.

V. CONCLUSION

In conclusion, we have demonstrated that NMR methods are capable of measuring the nonlocal dispersion coefficients $\widetilde{D}_{\parallel,\perp}(\mathbf{q},\omega)$. In the local (large time and distance) limit, our results agree with earlier measurements using more conventional methods and for no flow they agree qualitatively with a simple model of restricted diffusion. Our results with flow are in reasonable agreement with a calculation based on a dilute-sphere approximation to the medium, but the domain of validity of the latter is limited and further theoretical work is called for.

ACKNOWLEDGMENTS

This work was supported by NSF Grants Nos. DMR 9100044 and DMR 9501171.

[1] F. A. L. Dullien, *Porous Media: Fluid Transport and Pore Structure*, 2nd ed. (Academic, San Diego, 1992), Chap. 6.
[2] D. L. Koch and J. F. Brady, J. Fluid Mech. **180**, 387 (1987); Chem. Eng. Sci. **42**, 1377 (1987).
[3] J.-P. Hulin and D. Salin, in *Disorder and Mixing*, edited by E. Guyon, J.-P. Nadal, and Y. Pomeau (Kluwer Academic, Dordrecht, 1988), p. 89.
[4] P. T. Callaghan, D. MacGowan, K. J. Packer, and F. O. Zelaya, J. Magn. Reson. **90**, 177 (1990); P. T. Callaghan, A. Coy, D. MacGowan, K. J. Packer, and F. O. Zelaya, Nature **351**, 467 (1991).
[5] P. P. Mitra, P. N. Sen, L. M. Schwartz, and P. Le Doussal, Phys. Rev. Lett. **68**, 3555 (1992).
[6] M. D. Hürlimann, K. G. Helmer, L. L. Latour, and C. H. Sotak, J. Magn. Reson. A **111**, 169 (1994).
[7] P. T. Callaghan, *Principles of Nuclear Magnetic Resonance*

Microscopy (Clarendon, Oxford, 1991).
[8] R. M. Cotts, M. J. R. Hoch, T. Sun, and J. T. Markert, J. Magn. Reson. **83**, 252 (1989)
[9] A. Caprihan and E. Fukushima, Phys. Rep. **198**, 195 (1990).
[10] J. W. Hiby, in *Proceedings of the Symposium on Interactions Between Fluids and Particles*, edited by P. A. Rottenburg (Institution of Chemical Engineering, London, 1962), p. 312.
[11] P. G. Saffman, Fluid Mech. **7**, 194 (1960).
[12] A. Ding and D. Candela (unpublished).